

RESPONSE OF A BALLOON-BORNE OMNIDIRECTIONAL DETECTOR TO THE ATMOSPHERIC SECONDARY CHARGED COSMIC RADIATION AT A PLACE OF 11.5 GV GEOMAGNETIC CUT-OFF

I. N. Azcárate¹

Instituto Argentino de Radioastronomía, Argentina

Received 2000 October 30; accepted 2001 May 5

RESUMEN

Se describe un experimento llevado a cabo con un centelleador plástico de gran volumen. El sistema detector fue transportado por un globo estratosférico, que fue lanzado desde Reconquista, Provincia de Santa Fe, Argentina, el 24 de febrero de 1992. El corte geomagnético del lugar es 11.5 GV. Los espectros de pérdida de energía de la radiación gama (para $E_\gamma \geq 4.15$ MeV) y la componente cargada de la radiación cósmica secundaria fueron medidos —alternativamente— a diferentes alturas durante el ascenso del balón, y a la altura de nivelación. En un trabajo publicado anteriormente (Azcárate 2000) se analizó el espectro de radiación gama atmosférica. La forma de espectros de pérdida de energía debida a la radiación cargada puede explicarse, al menos cualitativamente, por el cálculo de la respuesta del detector a este tipo de radiación.

Se postula que, a altura de nivelación, el pico observado en el espectro se debe fundamentalmente a muones relativistas que inciden horizontalmente sobre el detector. Se ha obtenido también la curva de crecimiento para el conteo bajo el pico y la intensidad de los muones relativistas.

ABSTRACT

An experiment performed with a balloon-borne large plastic scintillator is described. The detector system was transported by a stratospheric balloon, that was launched from Reconquista, Provincia of Santa Fe, Argentina, on February 24, 1992. The geomagnetic cut-off of the site is 11.5 GV. The energy loss spectra of both the atmospheric gamma-radiation (for $E_\gamma \geq 4.15$ MeV) and the charged component of the secondary cosmic radiation were alternatively measured at different altitudes, during the ascent of the balloon, and at ceiling altitude. The atmospheric gamma-ray spectrum was analyzed in an earlier paper (Azcárate 2000). The shape of the energy loss spectrum due to charged radiation can be explained, at least qualitatively, by the computation of the response of the detector to this type of radiation.

It is argued that, at ceiling altitude, the observed feature in the spectrum is due mainly to relativistic muons inciding horizontally on the detector. The growth curve for the counting rate below the peak and the intensity of relativistic μ mesons are also obtained.

Key Words: **BALLOONS — INSTRUMENTATION: DETECTORS — INTERSTELLAR MEDIUM: COSMIC RAYS**

1. INTRODUCTION

Primary cosmic ray particles, when entering the Earth's atmosphere, interact with the atmospheric

nuclei and produce secondary particles. Among the primary cosmic rays, proton and helium nuclei are the major components, and they produce a large fraction of these secondary particles. Most of the secondary particles decay, and some of the decay

¹Member of the Carrera del Investigador Científico y Tecnológico of CONICET, Argentina.

products are muons. Muons are the decay products of π^- mesons. Other components of the secondary cosmic radiation are protons, electrons, X-rays, gamma-rays, and neutrons. To understand the physical processes from which the various components of the secondary cosmic radiation originate, and their propagation through the atmosphere, it is necessary to have a detailed knowledge of the intensity and energy distribution as a function of both the zenith angle and the atmospheric depth of the observations. There is also a dependence on the geomagnetic cut-off rigidity at the place of the measurement, which determines the minimum energy of the primary particles that incide on the top of the atmosphere.

By means of balloon-borne detectors, several observations of the secondary radiation have been made, but most of these have determined the intensity in the vertical direction. In the experiment referred to in this paper, and as a byproduct of the determination of the atmospheric gamma radiation spectrum (Azcárate 2000), energy loss spectra of the charged radiation were obtained at different altitudes, and their shapes are explained by computing the path length distribution of this type of radiation in the detector. In this paper, we refer basically to the response of the detector to the charged radiation.

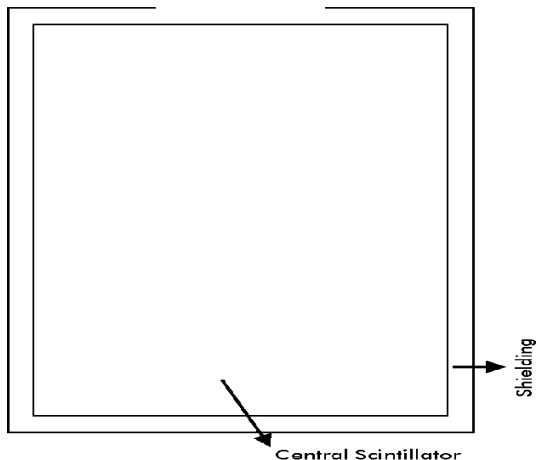


Fig. 1. Diagram of the detector system composed by a parallelepiped-shaped central scintillator with dimensions $16 \times 16 \times 24 \text{ cm}^3$ surrounded by a plastic scintillator 1 cm thick called the shielding.

2. THE DETECTOR SYSTEM

The equipment was transported to a height of about 30 km by a stratospheric balloon, launched from Reconquista, Provincia de Santa Fe, Argentina

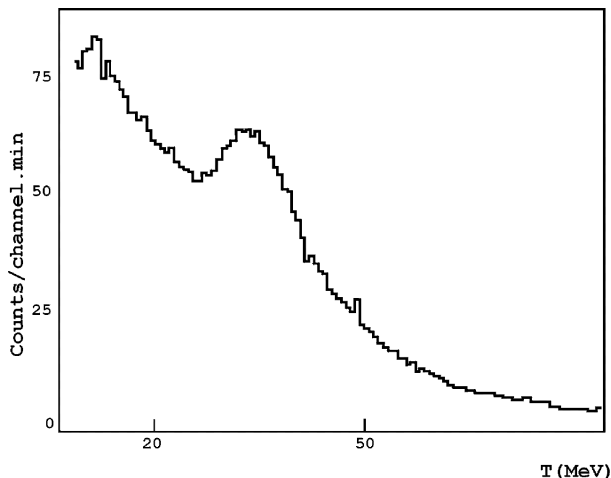


Fig. 2. Charged radiation energy-loss spectrum observed at 9.5 g cm^{-2} .

(a place with a geomagnetic cut-off of 11.5 GV) on 24 February 1992, and it reached a ceiling altitude of 9.5 g cm^{-2} , remaining at this altitude for about 5 hours. The detector system was composed of a parallelepiped-shaped plastic scintillator (polystyrene) of $16 \times 16 \times 24 \text{ cm}^3$, sensitive to neutral radiation (gamma-rays and neutrons) and charged particles, surrounded by a 1 cm thick layer of plastic scintillator that was used to veto the analysis of the pulses produced in the central detector by the charged particles that pass through both scintillators simultaneously. In Figure 1 a diagram of the detector system is shown. In this experiment, it was possible to select by telemetry one of the two modes of spectral analysis:

a) Mode veto-on: only the pulses of the central detector without the simultaneous presence of pulses in the external scintillator are analyzed.

b) Mode veto-off: the pulses recorded simultaneously with a signal from the external scintillator are included in the analysis. Since a simultaneous pulse in both scintillators is produced by charged particles that pass through them in the mode veto-off, pulses produced by neutral and charged radiation are analyzed, whereas in the mode veto-on, the charged radiation is eliminated almost completely (with an efficiency of ≈ 0.95), according to tests carried out at laboratory. In the following, the charged radiation spectra are shown and discussed.

3. CHARGED RADIATION SPECTRA

The spectra obtained in the mode veto-off include the pulses produced by the charged particles that traverse the central scintillator. By subtract-

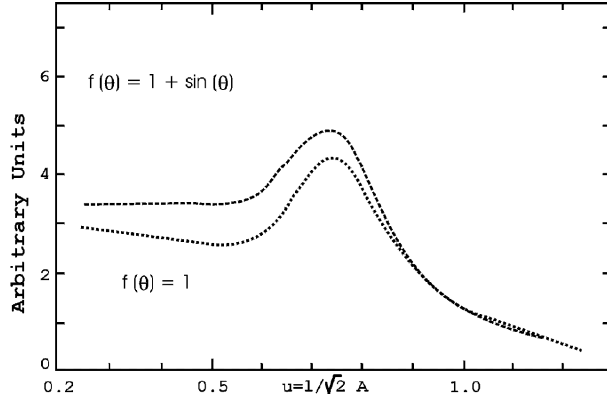


Fig. 3. Pathlength distribution in the central detector for particles that completely traverse it, computed for two angular distributions, $f(\theta) = 1$ and $f(\theta) = 1 + \sin(\theta)$, as a function of $u = l/\sqrt{2} A$ (where l is the traversed path and $A = 16$ cm is the longitude of the detector minor dimension). Both distributions have been corrected for the detector resolution.

ing from this total spectrum that of the neutral radiation observed in the mode veto-on, the energy-loss spectrum resulting only from the charged particles is obtained. Allowing for the dependence between the light-signal and the energy deposited by particles of different classes, the detection thresholds for electrons, muons, and protons are 4.15, 6.0, and 10.0 MeV, respectively. The shape of one of the energy-loss spectra of charged radiation obtained at ceiling altitude is shown in Figure 2. Its most characteristic feature is the presence of a peak in the spectrum that corresponds to a deposited energy in the scintillator of approximately 32 MeV.

At sea-level, where the high energy charged radiation (composed mainly of μ mesons) depends on the zenith angle θ following a law $f(\theta) \propto \cos^2\theta$, the energy-loss spectrum measured with the same detector shows two maxima (Duro, Ghielmetti, & Azcárate 1976). The presence of these two maxima is explained by computing the distribution of the energy deposited in the central scintillator by particles traversing it completely, when both the angular distribution $\propto \cos^2\theta$ and the path length distribution in the parallelepiped detector are taken into account.

The presence of only one peak at ceiling altitude clearly indicates a change of the angular distribution of the charged radiation, as compared with sea-level. The computation of the pathlength distribution in the detector (Gandolfi 1970) for isotropic incidence $f(\theta) = 1$, when the resolution of the detector is taken into account, gives as a result the presence of only one peak. The same result is obtained for distribu-

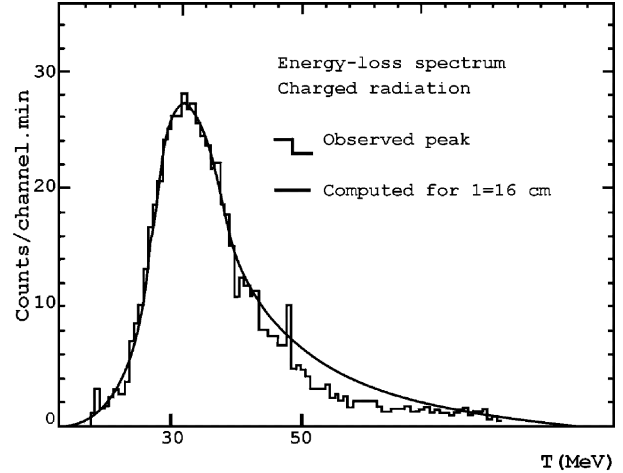


Fig. 4. Peak shape obtained at 9.5 g cm^{-2} after subtracting the continuum background from the observed charged radiation spectrum. It is compared with the theoretical energy-loss distribution for minimum ionization μ mesons that traverse 16 cm of polystyrene.

tions for which the intensity increases with the zenith angle (as an example $f(\theta) = 1 + \sin\theta$, see Figure 3). For both cases, the peak position is almost coincident, and corresponds to a longitude of 16 cm, which is that of a particle inciding perpendicularly on the lateral faces of the scintillator. Since the detector was used with the largest dimension in the vertical position, that longitude implies horizontal incidence. I compare in Figure 4 the observed peak with the computed energy-loss spectrum produced by minimum ionization muons ($E_\mu \simeq 320 \text{ MeV}$) when traversing 16 cm of polystyrene, allowing for fluctuations in the ionization by collisions (Rossi 1952) and statistical fluctuations in the detection process of scintillation. The observed peak was obtained by subtracting the extrapolated background, assuming continuity in the energy spectrum. The very good agreement between the two curves seems to indicate that the particles producing the peak are muons with energies of hundreds of MeV, coming from a horizontal direction. A similar computation for protons gives equivalent results, but it is possible to exclude this component, as well as electrons, as significant contributors to the peak (see the point on the detector response to charged radiation). From the energy-loss charged radiation spectra obtained in the mode veto-off during the ascent of the balloon, the counting rates "below the peak" as a function of the atmospheric depth have been derived. This growth curve (Figure 5) has a maximum at about 55 g cm^{-2} . In

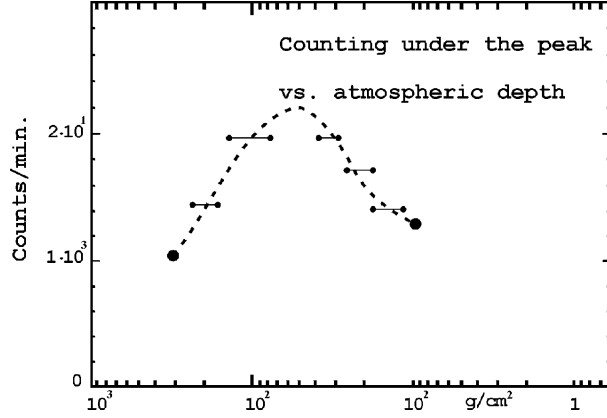


Fig. 5. Growth curve of the counting rate below the peak, as a function of atmospheric depth.

a different measurement of the zenith distribution of the charged secondary cosmic radiation, made with omnidirectional telescopes at a place of geomagnetic cut-off 10.6 GV (Aragón, Gagliardini, & Ghielmetti 1977), it is found that the horizontal intensity has a maximum at an atmospheric depth of 42 g cm^{-2} . The similar shapes of both growth curves support the hypothesis that the observed peak is produced by particles inciding horizontally on the detector.

Finally, by computing the geometric factor of the detector for particles with pathlengths corresponding to the maximum of the pathlength distribution, assuming efficiency equal to unity for charged particle detection, and disregarding the proton and electron contribution, it is possible to give an approximate estimate for the horizontal intensity of the relativistic μ mesons ($E_\mu > 300 \text{ MeV}$) which is $\sim 10^{-2} \mu$ mesons $\text{cm}^{-2} \text{ s}^{-1} \text{ ster}^{-1}$.

4. DETECTOR RESPONSE TO CHARGED RADIATION

The charged particles incident on the detector at ceiling altitude (9.5 g cm^{-2}) are mainly electrons, protons, and muons. The pulse spectrum produced in the detector for each of these components depends on its unidirectional energy spectrum, that is to say, the energy distribution and its variation with the zenith angle. Furthermore, for each point P and incidence direction (θ, ϕ) , there is a maximum pathlength $l(P, \theta, \phi)$ to be traversed in the detector. This pathlength may be greater or less than the particle range. Therefore, the particle may deposit all or part of its initial energy. The relationship between the deposited and incident energies, T and E , is a function of the distance traversed by the particle in

the scintillator material. Neglecting the radiation losses (which can be considered zero for protons and μ mesons) the relationship is

$$T(E, X) = \int_0^X (dE/dx)_{col} dx ,$$

if $l < R(E)$, and $T(E, X) = E$ if $l > R(E)$. Here, $X = \rho l$ and ρ is the material density, dE/dx_{col} is the average energy-loss due to collisions per unit pathlength ($\text{MeV cm}^{-2} \text{ g}^{-1}$) that a particle experiences in the material and $R(E)$ is the range corresponding to the initial energy. For protons and muons $E(dE/dx)_{col}$ exhibits a flat minimum for the ranges of some GeV and hundreds of MeV, respectively (Berger & Seltzer 1964a,b).

To compute the pulse spectrum dN/dT for each component, I had to consider the pathlength distribution in the detector. For each of the three components, the following expression was calculated

$$((dN/dT)dT) = A1 + A2 ,$$

where

$$A1 = \int_{E_1}^{E_2} (dji/dE)dE \int_{R(E)}^{lM} (dG/dl)dl ,$$

and

$$A2 = \int_{R(E)}^{lm(T)} (B1 + B2)(dG/dl)dl ,$$

with

$$B1 = \int_{E_3}^{E_4} (dji/dE)dE ,$$

and

$$B2 = \int_{E_5}^{E_6} (dji/dE)dE .$$

Here, dN/dT is the number of pulses with energies between T and $T+dT$, dji/dE is the differential spectrum of the incident particles, lM is the greatest diagonal of the parallelepiped, and dG/dl is the differential geometric factor.

The first term $A1$ in the second member of the computation of $(dN/dT)dT$ includes the contribution to this energy range of the particles that stop in the scintillator (low energy particles). The second term $A2$ corresponds to those particles that pass through the scintillator (relatively high energy particles) with pathlengths in the detector between $l = R(E)$ and $l = lm(T)$. This last value of l depends on the range T , $T+dT$ being considered. The relationship between T and E , for X values varying by

steps of 1 g cm^{-2} , has been calculated for the three components, and curves like those shown in Figure 6, corresponding to μ mesons, have been obtained. For a given interval T , $T+dT$ the curves $T(E,x)$ allow us to estimate the limits of the integrals appearing in the second member (E_1 to E_6). Regretfully, the information about the differential spectra dji/dE and their dependence on the zenith angle is rather sparse, since most of the spectral measurements have been made for radiation incident from the vertical direction. For this reason, I had to estimate the pulse spectra by assuming an isotropic angular distribution and the following spectral shapes. (a) For protons, spectrum measured in the vertical direction with a value of 4.3 GV for the geomagnetic cut-off and an atmospheric depth of 5 g cm^{-2} (Bellotti et al. 1999). (b) For electrons, a computed spectrum for the vertical direction, with values $\propto 10 \text{ GV}$ and 10 g cm^{-2} (Daniel & Stephens 1974). (c) For μ mesons, a measured spectrum for the vertical direction, with values of 4.3 GV and 5 g cm^{-2} (Bellotti et al. 1999).

In Figure 7, we show the energy-loss spectra in the detector computed for the three components. Some differences are evident, although in all three cases only one peak with energies between 30 and 40 MeV appears in the spectra. This peak is determined by the predominance of the second term in the calculation of dN/dT , which corresponds to high energy particles. In the case of muons, the shape of the peak is very similar to the observed one.

5. CONSIDERATIONS ABOUT THE RELATIVE CONTRIBUTION OF EACH COMPONENT TO THE FEATURE IN THE SPECTRUM

Due to the rapid decrease of the proton intensity with the thickness of the traversed air layer (Rossi 1952), a considerably lower intensity in the horizontal direction as compared to the vertical intensity is to be expected, since the protons incident horizontally on the detector must traverse about 300 g cm^{-2} for the ceiling altitude of 9.5 g cm^{-2} . The computed intensity for μ mesons for zenith angles near 90° (horizontal incidence) is several times greater than that corresponding to the vertical direction (Okuda & Yamamoto 1965). The same authors show that a zenith angle distribution with a maximum in the horizontal direction is valid for electrons. From these qualitative considerations, I argue that the possibility that the protons are responsible for the appearance of the peak may be disregarded.

Another qualitative argument allows us to neglect the electron contribution to the peak. In the computation that leads to the curves $T(E,x)$ for elec-

trons, only the $(dE/dx)_{col}$ have been considered. The radiation energy losses $(dE/dx)_{rad}$ have been neglected. However, this term can be important for energies starting at some tens of MeV, and predominates for energies greater than 100 MeV. Therefore, both the average energy loss per unit pathlength, and the deposited energy T for a given pathlength l , will be considerably greater than those used in the computation. To illustrate this, let us consider a particular case: allowing only for the collisional energy losses, electrons of 50 and 80 MeV would deposit in the scintillator (for a longitude of 16 cm) an energy very close to 32 MeV, and they would contribute to the feature in the spectrum. But if the radiation energy losses are taken into account, the deposited energies would be 46 and 61 MeV, respectively. The analysis of the radiation losses demands a much more complicated computation but, again, a qualitative discussion indicates that its inclusion would lead to the smearing out and disappearance of the feature, as a result of the fast increase of the energy given to the medium as a function of the incident electron energy. Therefore, the hypothesis is made that the presence of the peak in the charged radiation spectrum is due essentially to relativistic μ mesons incident horizontally on the detector, and having an intensity

$$I \approx 10^{-2} \mu - \text{mesons cm}^{-2} \text{ s}^{-1} \text{ ster}^{-1} .$$

6. CONCLUDING REMARKS

(a) In the experiment reported in this paper, the energy-loss spectra of the secondary charged cosmic-ray particles entering the central scintillator were registered in mode veto-off, both during the ascent of the balloon and at ceiling altitude.

(b) The main feature of the spectra at ceiling altitude is the presence of a peak. This peak is explained by the computation of the response of the detector to incident charged particles traversing the central scintillator.

(c) By means of qualitative arguments, the hypothesis is put forward that this feature is mainly due to relativistic muons incident horizontally on the detector, which would imply an angular distribution of atmospheric muons at 9.5 g cm^{-2} peaked in the horizontal direction.

This research has been partially supported by grant PIP 0430/98 from the National Scientific and Technological Council (CONICET), from Argentina. I. N. Azcárate is a member of the Carrera del Investigador Científico y Tecnológico of CONICET.

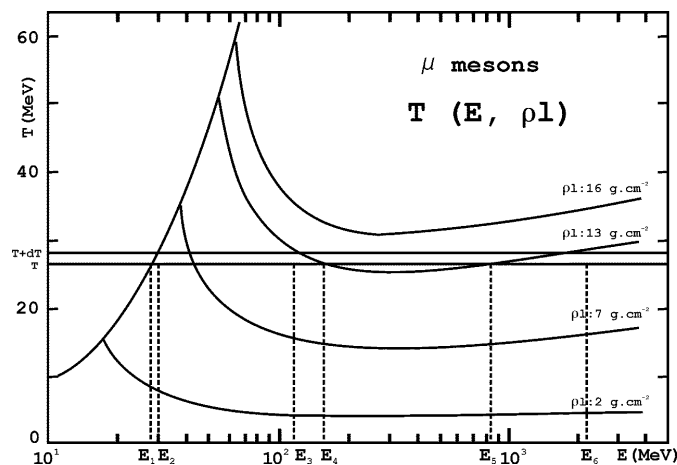


Fig. 6. Typical shape of the curves that represent $T(E,x)$ for μ mesons in polystyrene.

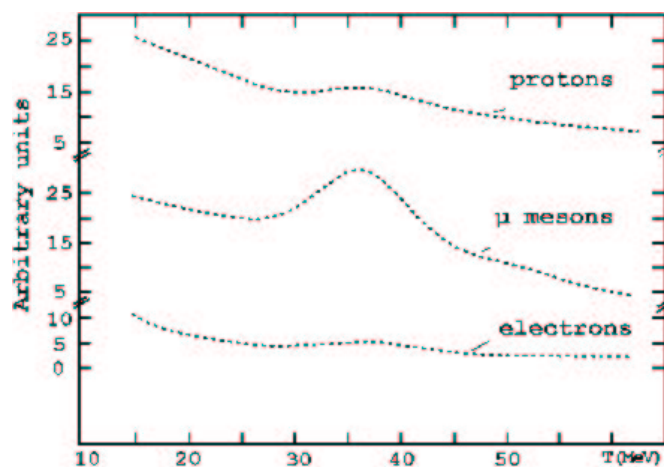


Fig. 7. Energy-loss spectra in the detector computed for electrons, μ mesons, and protons, with isotropic incidence and the spectral distributions given in the papers quoted in the text.

REFERENCES

- Aragón, G., Gagliardini, A., & Ghielmetti, H. S. 1977, Sbarro Bulletin, 6, 243
 Azcárate, I. N. 2000, RevMexAA, 36, 81
 Berger, M. J., & Seltzer, S. M. 1964a, NASA SP-3012
 ————. 1964b, NASA SP-3113
 Bellotti, R., et al. 1999, Phys. Rev. D, 60, 052002
 Daniel, R. R., & Stephens, S. A. 1974, Rev. of Geophys. and Space Phys., 12, 233

- Duro, J. C., Ghielmetti, H. S., & Azcárate, I. N. 1976, Características de un centelleador plástico paralelepípedo, IAFE, PC-1-76
 Gandolfi, E. 1970, Cálculo de la distribución de caminos en un detector cilíndrico, Centro Nacional de Radiación Cósmica, PI-1-70
 Okuda, H., & Yamamoto, Y. 1965, Report of Ionosphere and Space Research in Japan, 19, 322
 Rossi, B. 1952, High Energy Particles (New York: Prentice-Hall Inc.)

Ismael N. Azcárate: Instituto Argentino de Radioastronomía, Casilla de Correo No. 5, (1894) Villa Elisa, Bs. As., Argentina (azcarate@irma.iar.unlp.edu.ar).